Development of a Structural Integrity Assessment Methodology for a Steel Surface Tank

By

Gladys H. Albert

Thesis
Submitted to Flinders University
for the degree of

MEMC Master of Engineering (Mechanical)

College of Science and Engineering

23 May 2024

TABLE OF CONTENTS

ABSTRACT

This project investigated the structural integrity of steel surface tanks, specifically those used for storing hazardous substances, utilising non-destructive testing (NDT) techniques and finite element analysis (FEA). The primary objective is to integrate phased array ultrasonic thickness measurements into comprehensive shell and solid finite element models to evaluate stress distributions, identify critical areas of concern, and ensure compliance with industry standards.

To achieve this, MATLAB code was developed to process the data, create a detailed 3D representation of wall loss, and calculate the tank's fill capacity based on structural integrity. The MATLAB code handles data extraction and conversion, producing visualisations that highlight areas with significant thickness loss. These visualisations aid in assessing the tank's structural health and pinpointing areas that may require maintenance.

The analysis compares the shell finite element model with a solid finite element model to validate the shell model's accuracy and computational efficiency. While the shell model offers computational benefits and is suitable for preliminary assessments, the solid model provides detailed stress and deformation patterns, particularly in regions with significant thickness variations. The use of shell modelling enhances computational efficiency and Compliance assessments is done with calculation of the factor of safety for assessment, making it feasible to analyse the entire structure and account for multiple corrosion sites and structural loading conditions, thereby increasing the reliability of the structural integrity assessment.

The project results underscore the importance of accurate data mapping and the use of advanced modelling techniques for reliable structural assessments. By integrating NDT and FEA, the study provides a framework for guiding maintenance and safety protocols for steel surface tanks, ensuring their longevity and safe operation. The insights gained from this project have the potential to revolutionise the prevention and management of tank failures, significantly benefiting industry partners.

DECLARATION

I certify that this thesis:
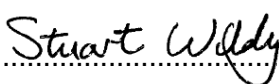
1. does not incorporate without acknowledgment any material previously submitted for a degree or diploma in any university

2. and the research within will not be submitted for any other future degree or diploma without the permission of Flinders University; and

3. to the best of my knowledge and belief, does not contain any material previously published or written by another person except where due reference is made in the text.

Signature of student.... *Gladys* ....

Print name of student.... Gladys Hyelni Albert..

Date.........06/06/2024..

I certify that I have read this thesis. In my opinion it is fully adequate, in scope and in quality, as a thesis for the degree of Master of Engineering (Mechanical). Furthermore, I confirm that I have provided feedback on this thesis and the student has implemented it fully.

Signature of Principal Supervisor......... *Stuart Wildy* ....

Print name of Principal Supervisor........Dr Stuart Wildy...................

Date.......19/08/2024...

ACKNOWLEDGEMENTS

LIST OF FIGURES

LIST OF TABLES

1. INTRODUCTION

The assessment of the structural integrity of steel tanks is crucial to prevent potential accidents and ensure the safe storage of substances like ammonia and other hazardous materials (Ojha & Dhiman 2010). Given the significant risks to human health and the environment in the event of a failure in processing storage tanks, the methodologies used to assess structural integrity must provide a realistic evaluation. Therefore, any structural integrity assessment must be based on data from non-destructive testing techniques that can provide information on the condition of the structure (Hassani and Dackermann 2023). For steel surface tanks, the use of ultrasonic testing has gained prominence for its ability to be able to measure the thickness of tank walls and detect defects, such as cracks, pitting corrosion, and other anomalies (Thakur and Kumar 2021) However, structural integrity assessment is also reliant on the modelling methodology that is utilised.

One approach to assess the integrity of a corroded structure is to perform finite element analysis using solid finite elements. However, modelling thin-walled structures using solid finite elements requires significant computational effort and is usually limited to modelling smaller areas of interest (Wang 2021). Alternatively, the use of shell finite elements to model thin-walled structures offers increased computational efficiency (Zhu et al. 2023). This allows for the entire structure to be analysed, accounting for loading conditions, structural constraints, and localised corrosion thickness losses.

Zhu et al. (2023b) and Sultana et al. (2015) investigated the use of shell finite elements to model corrosion in thin-walled structures. However, little progress has been made in modelling corroded real-world structures, such as a steel surface ammonia tank, using shell finite elements and requires further investigation.

This project aims to develop a methodology to utilise phased array ultrasonic thickness data for creating a shell finite element model to evaluate the stresses and structural integrity of steel surface tanks. The objectives of this project are detailed in the phases below:

Phase 1: Extraction and processing of ultrasonic wall thickness loss data from a steel surface storage tank to be used for the development of the finite element model.

Phase 2: Develop and validate a shell and solid finite element model in ANSYS, ensuring accurate stress distributions through mesh refinement studies.

Phase 3: This phase is to evaluate the structural integrity of the steel surface storage tank based on the finite element shell model and compare the results to the AIP standard 653 (American Petroleum Institute 2001).

In line with these phases, phased array ultrasonic thickness (PAUT) corrosion mapping was carried out on four cardinal points (North, South, West, and East) of the 4241 TK1000 Flotation Feed Tank Neutral Pulp at BHP Olympic Dam in late 2020. This mapping aimed to detect any degradation or corrosion. The collected data will be used to create a shell finite element model to evaluate the tank's stresses and structural integrity. MATLAB code will be employed to extract full-field thickness data from the PAUT corrosion mapping of the tank.

Using the data, along with internal tank pressure and loading conditions, an ANSYS script will be created to develop a shell finite element model. This model will efficiently simulate stress distributions due to thickness losses. The shell finite element model must produce realistic stress distributions within the structure and near areas of corrosion. The mesh of the finite element model must achieve mesh convergence to be considered valid. This model can then be used in the structural integrity assessment of the entire tank.

The findings of this project will contribute to developing a methodology that enables reliability engineers to perform improved structural analysis of tanks using ultrasonic thickness measurements, making this approach faster and more efficient.

1.1 Scope of the research

The scope of this project is to develop a methodology that can be used to assess the integrity of surface tanks in line with the phases listed in the project objectives above. This project is specifically designed to exclude the assessment of stress corrosion cracking (SCC) and residual stress analysis (RSA). While both SCC and RSA are important considerations in the structural integrity assessment of steel tanks, they are not within the scope of this research endeavour. Instead, the primary focus of this project is on directly comparing stress data provided by the industry partner BHP across a range of simulated conditions. The exclusion of SCC and RSA allows for a more focused examination of stress distribution and its impact on structural integrity, providing valuable insights to inform future tank design and maintenance strategies.

1.2   Thesis Outline

Chapter 1: Introduction:

Chapter 2: Literature Review:

This chapter reviews studies on the effects of corrosion, with a particular focus on pitting corrosion. It also examines advancements in corrosion assessment techniques, especially non-destructive methods like ultrasonic testing. Additionally, it provides a comparative analysis of finite element models, discussing the use of shell versus solid models in structural analysis. The integration of Phased Array Ultrasonic Testing (PAUT) with Finite Element Analysis (FEA) is also reviewed, highlighting studies that combine corrosion mapping with structural modeling.

Chapter 3: Methodology

This chapter describes the process of PAUT corrosion mapping and data acquisition. It outlines the steps for processing corrosion data using MATLAB. The development and validation of shell and solid finite element models in ANSYS are detailed, followed by a methodology for comparing different finite element models and evaluating their effectiveness.

Chapter 4: Results and Discussion

This chapter presents detailed results from the shell and solid finite element models. It includes an analysis of structural integrity and discusses the implications of the findings for tank safety. The results are validated against industry standards, with a discussion on how they comply with or deviate from existing standards.

Chapter 5: Conclusions and Recommendations:

This chapter summarizes the critical findings and their significance. It discusses the implications for the industry and how this research can change or reinforce current practices. Finally, it offers suggestions for future research to expand on or refine the current work.

References: Comprehensive list of all sources cited throughout the thesis.

2. LITERATURE REVIEW

The structural integrity of steel surface tanks, essential for containing hazardous substances, is significantly threatened by corrosion. Pitting corrosion poses a severe challenge due to its localised nature, creating deep cavities on metal surfaces and compromising tank safety and functionality (Nakai, Matsushita, & Yamamoto 2006). This review aims to explore the complexities of corrosion, focusing on pitting corrosion, and examines advancements in ultrasonic testing and finite element analysis (FEA) for improving structural integrity assessments.

Recent developments in PAUT corrosion mapping have become crucial in non-destructive evaluation of steel tanks, offering reliable detection of pitting corrosion and thickness loss. The precision and reliability of this technique are vital for maintenance and safety protocols, emphasizing the need for continuous advancements in ultrasonic technology and operator training (Industry Standard Organisation, 2020). Ilman et al. (2020) highlighted those recent advancements in structural analysis using FEA, particularly shell finite element models (SFEMs), have enabled the evaluation of corrosion impact on large, thin-walled structures. SFEMs provide computational efficiency and analytical depth, accurately modelling localised corrosion patterns and predicting strength reduction due to corrosion-induced surface damage.

However, accurately capturing the complex geometries and stress states induced by corrosion remains challenging, necessitating refined modelling techniques and validation against real-world data. Zhu et al. (2024) integrated PAUT corrosion mapping data with FEA for subsea pipelines, improving accuracy, enhancing safety, and extending asset lifespan. Their work contributes to effective corrosion management strategies. This review aims to provide a comprehensive understanding of corrosion's impact on steel tanks, contributing to the development of more effective strategies for ensuring the safety and longevity of these infrastructures. The synthesis of the studies included in this review are categorised into four key themes.

2.1 The Impact of Corrosion

Ilman et al. (2020) emphasised the significant reduction in material durability due to corrosion under service loads, highlighting the impact of corrosion-stress interactions on the topological features and ultimate strength of large-scale steel structures. In contrast, Nakai et al. (2006) focused on the effect of pitting corrosion on the strength of web plates subjected to patch loading. Their findings demonstrate that pitting corrosion significantly weakens structural components, a point that Ilman et al. (2020) also underscored in their study.

However, both studies converge on the need for preventive measures. Ilman et al. (2020) recommended the development of advanced corrosion-resistant materials, whilst Nakai et al. (2006) advocated for regular inspections and maintenance. These recommendations underscore the

importance of addressing corrosion-stress interactions and implementing preventive measures to maintain the durability and safety of steel structures. Future studies should focus on these areas to further enhance our understanding of corrosion's impact on steel tanks and develop more effective strategies for ensuring their safety and longevity.

2.2 Corrosion Assessment Techniques

Silva et al. (2013) conducted an ultimate strength assessment of rectangular steel plates subjected to a random localised corrosion degradation. They employed both experimental and numerical methods to validate their findings, expressing that the combination of these methodologies provides a more comprehensive understanding of the structural integrity of corroded plates. This approach allowed for a more accurate representation of the corrosion process, capturing the non-linear, randomly distributed nature of corrosion. In contrast, Slater et al. (2000) conducted a finite element analysis of buckling in corroded plates. They emphasised the importance of using realistic corrosion patterns in simulations to improve predictive accuracy. The authors recommended the integration of advanced modelling techniques to better replicate real-world corrosion scenarios. These approaches contribute significantly to our understanding of corrosion's impact on steel structures and the development of effective strategies for their maintenance and preservation.

2.3 Finite Element Analysis: Shell vs. Solid Models

Wagner et al. (2018) argue that while solid models offer detailed insights, shell models provide a more efficient approach for large-scale simulations. This efficiency is crucial when dealing with complex structures and large data sets. On the other hand, Sultana et al. (2015) presents a comparative analysis of both shell and solid FEA models, demonstrating that the choice of modelling approach depends on the specific requirements of the structural analysis. These studies collectively highlight the importance of selecting the appropriate modelling approach in FEA. While Wagner et al. (2018) advocate for the efficiency of shell models, Sultana et al. (2015) emphasize the need for a tailored approach, considering the specific requirements of the structural analysis. This comparison underscores the complexity of FEA and the need for careful consideration in choosing the most suitable modelling approach.

2.4 Integrating PAUT Corrosion Mapping Data with FEA

Wang et al. (2021) used an improved 3D cellular automaton integrated with FEA to examine the effect of pit shape on pitted plates. This approach allowed for a more accurate prediction of the structural performance of corroded plates. On the other hand, Zhang et al. (2017) conducted an ultimate strength experiment of hull structural stiffened plates with pitting corrosion damage under uniaxial compression. They used FEA to enhance the reliability of their simulations, recommending this integrated approach for more accurate assessments of structural integrity. These studies highlight the importance of integrating PAUT corrosion mapping data with FEA for accurate

assessments of structural integrity, each focusing on different aspects of corrosion's impact on steel structures.

2.5 Technical Challenges and Future Directions

Zhao et al. (2018) and Zhu et al. (2020) both addressed technical challenges in corrosion modelling, with a focus on the bending capacity of corroded welded hollow spherical joints and the buckling of spherical shells with pitting corrosion, respectively. They collectively underscored the need for advanced modelling techniques and an improved understanding of corrosion patterns for accurate corrosion effect modelling. Furthermore, Zhu et al. (2020) emphasised the importance of future research focusing on the development of more sophisticated models. This collective insight highlights the importance of addressing technical challenges in corrosion modelling and the need for continuous research in this area, with a focus on the development of advanced modelling techniques and a deeper understanding of corrosion patterns.

2.6 Project Gap:

Despite advancements in PAUT corrosion mapping and FEA methodologies, a gap exists in developing a methodology that integrates these techniques for assessing steel surface tank integrity. Current research primarily compares shell and solid finite element models, overlooking the benefits of a cohesive framework. This lack of integrated approaches limits accurate prediction of localised corrosion effects on structural integrity. Addressing these gaps is crucial for advancing corrosion assessment and ensuring steel surface tank safety. The proposed project aims to develop protocols for integrating ultrasonic testing data with FEA and conduct validation studies. This will fill critical gaps in current methodologies and provide reliable tools for assessing and mitigating corrosion-induced risks.

3. DATA PROCESSING AND STANDARD EVALUATION

3.1 Methodology

The methodology employed in this project involves the utilisation of MATLAB for data processing and visualisation, aimed at constructing a 3D representation of tank wall loss based on PAUT corrosion mapping data. The project begins with data collection from industry partners, focusing on acquiring essential information such as tank geometry, material properties, and PAUT corrosion mapping data. Subsequently, MATLAB is utilised to process the acquired data and prepare it for seamless integration into ANSYS for finite element modelling to enable accurate representation of the tank structure in the subsequent phases of the project.

3.2 Corrosion Mapping and Damage Assessment

In late 2020, Phased Array Ultrasonic Testing (PAUT) corrosion mapping was conducted on four cardinal points (North, South, West, and East) of the 4241 TK1000 Flotation Feed Tank Neutral Pulp to evaluate the presence of degradation or corrosion. Typically, each section of the tank was examined in 600 mm intervals. The report includes a general image of the corrosion map covering all scans, illustrated in Figure 1. Certain parts of the corrosion map lack data, indicated by grey or black sections, scan areas that were inaccessible due to obstructions such as pipes, doors and some other structures during the assessment. The absence of data in these areas requires careful consideration in the model. The spreadsheet provided by industry partner provides details about the minimum wall thickness for each scanned area. However, the raw full-field PAUT scan data was not available. Therefore, to replicate the tank's thickness loss, data had to be extracted from the corrosion overview map in Figure 1, utilising the map's colour scale, as depicted in **Error! Reference source not found.**.
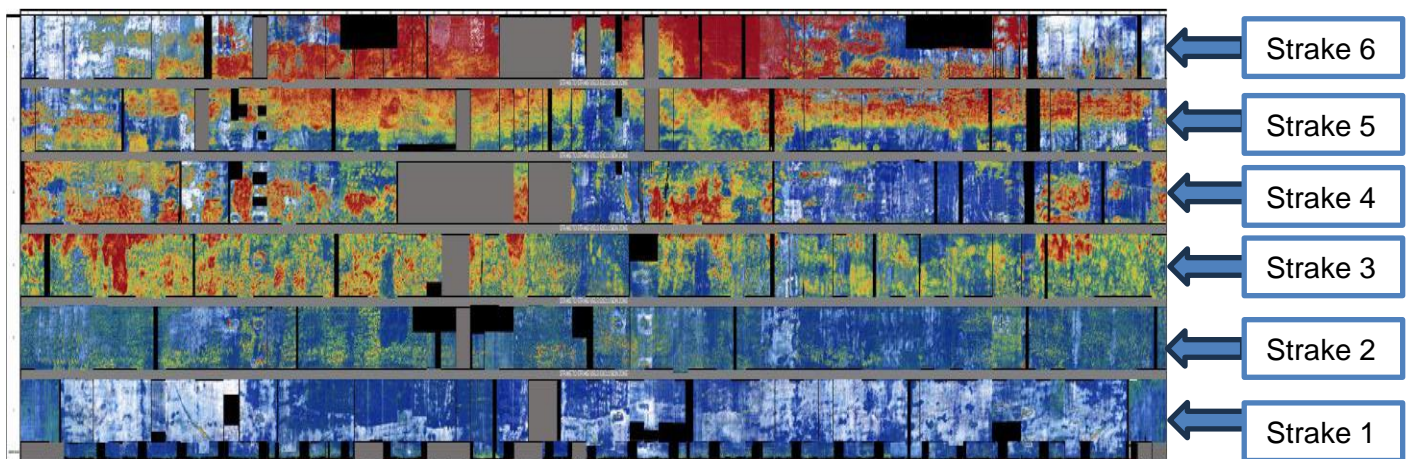
Figure 1: Corrosion map overview.

(a)   (b)
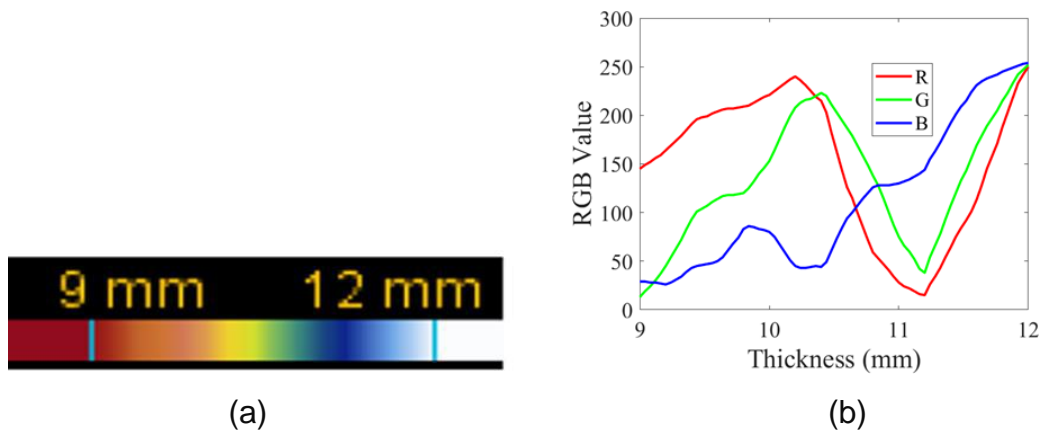
Figure 2: (a) is the Colour scale of the corrosion map overview image and (b) is the colour scale in converted to RGB colour values
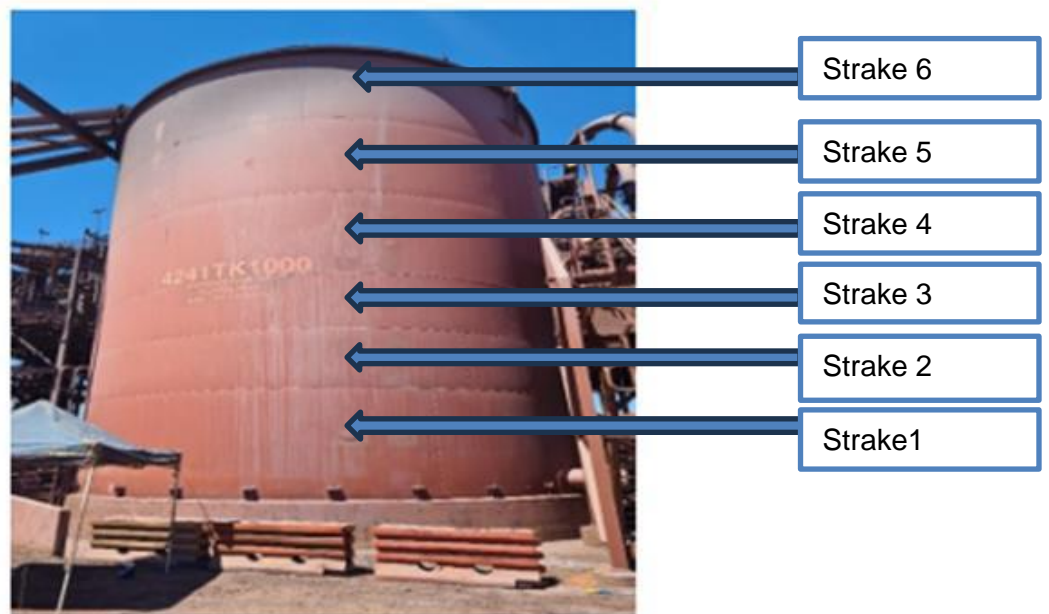
Figure 3: Overview of the tank

3.3 Data Collection and Processing

The spreadsheet provided by industry partner provides details about the minimum wall thickness serving as the primary source for conducting further analysis. This analysis involved extracting thickness information from corrosion map overview Figure 1 utilising the colour scale in **Error! Reference source not found.**a, to create a detailed visualisation of the extent of wall loss observed across the tank. The extracted thickness information from the images enabled the creation of detailed visualisations, such as 3D representations or heatmaps, to depict the distribution of wall loss across different sections of the tank in MATLAB to be assess for further analysis. An issue was found with utilising the corrosion mapping overview in Figure 1 which shows that the strakes of the tank were not scale properly. To address this issue, the image was rescaled using a MATLAB script to ensure the strakes in the corrosion map image reflect the actual dimensions of the tank, which can be seen in Figure 3.
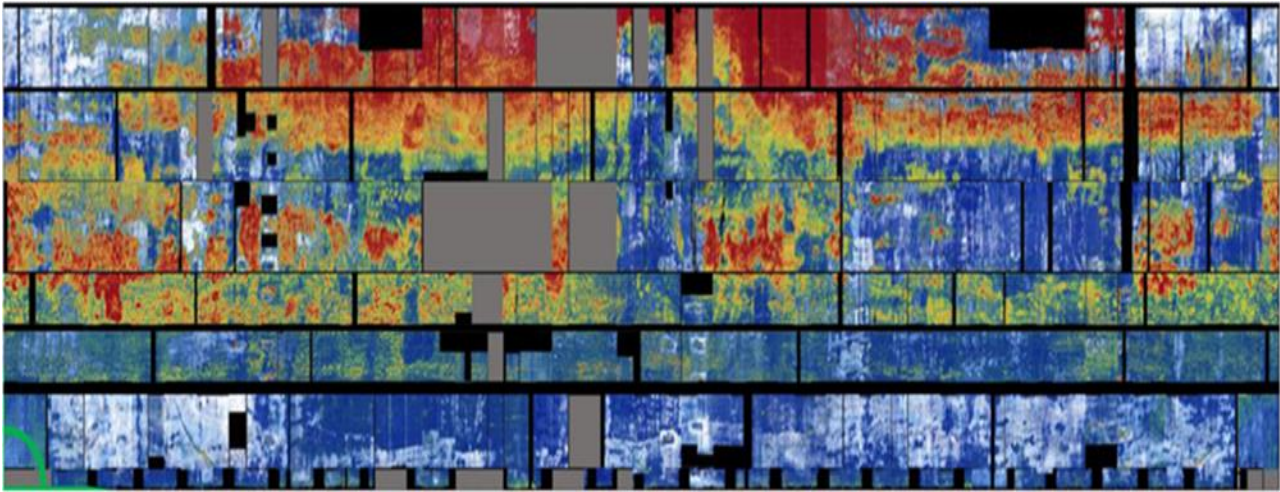
Figure 4:The rescaled image of the corrosion map.

Following the rescaling process, another issue was discovered that the minimum wall thickness loss measurement data for each of the section scanned on the spreadsheet has major inconsistencies concerning the starts of the scan and the end of the scan location and to validate these scan locations against the corrosion map overview in Figure 1. Adjustments were made to the data to enhance the dataset's completeness and accuracy. As a result of these adjustments, the minimum wall thickness loss of the tank for each scan area is plotted on top of the rescaled corrosion map overview image to ensure scan areas align. The data is now fully integrated into the visualisation process as seen in Figure 5
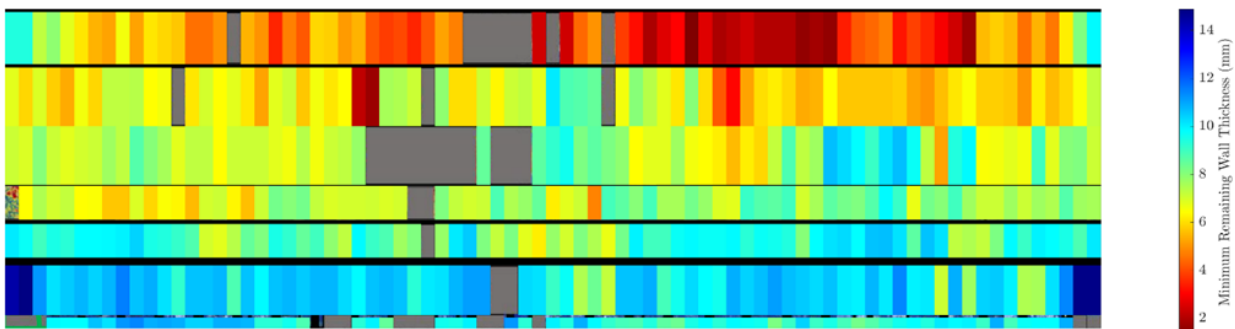
Figure 5:Minimum wall thickness loss of the tank for each scan area plotted on top of the rescaled corrosion map overview image

3.4 Mapping Data for Modification

To effectively address gaps in the dataset, particularly concerning tank wall thickness measurements from the start and the end location once validated, a MATLAB script was then developed to map the thickness associated with the RGB colour values to the corrosion overview map RGB image in **Error! Reference source not found.**b. The script also removed areas that did not include scan data, such as the grey and black areas in the image and the mean value of the wall thickness data was chosen

9

to be filled in with appropriate thickness values before importation into ANSYS model in the fallowing chapter. The extracted wall thickness loss data from the corrosion map image and the filled gap data can be seen in **Error! Reference source not found.**.
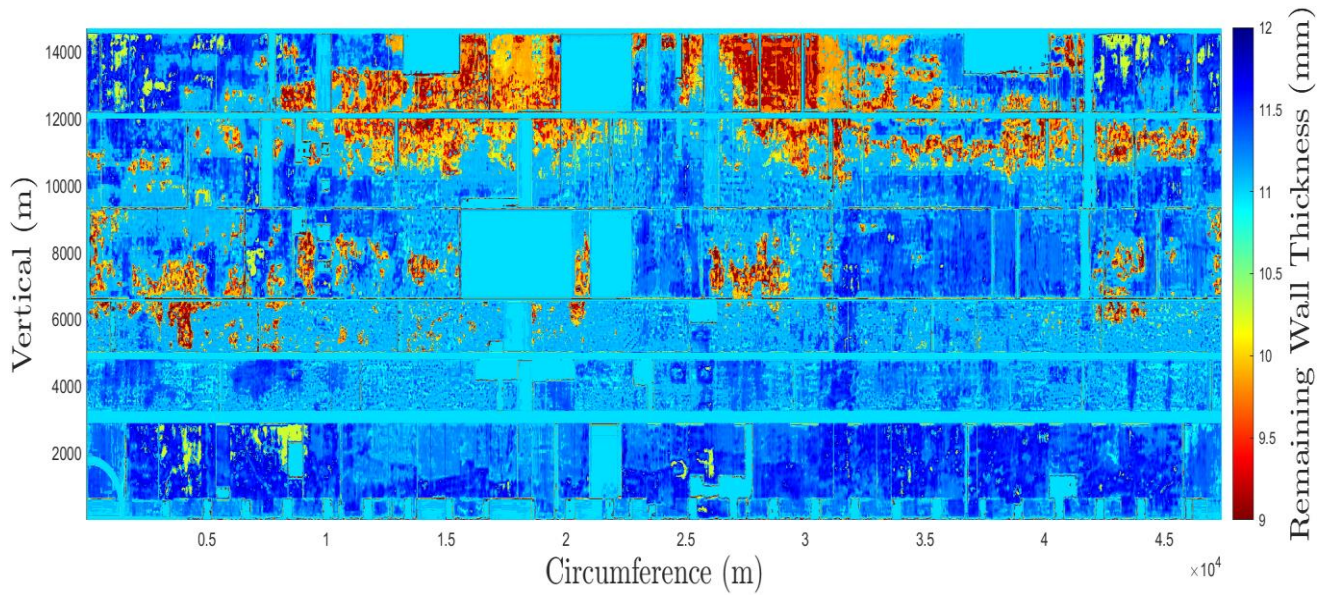
Figure 6:Extracted wall thickness data from the corrosion map overview image with the filled in data.

4. SHELL/SOLID MODELLING AND MESH VALIDATION

The second phase of the project focuses on developing and validating a shell finite element model (FEM) for the tank using ANSYS. This phase analyses a shell with 12mm nominal wall thickness, which is essential for ensuring structural integrity under various loading conditions and a shell with the imported minimum wall thickness loss data provided by industry partners. The main goal is to achieve a converged shell finite element mesh that accurately predicts the tank's stress distributions by applying material properties, load conditions, and conducting a mesh refinement study, with a focus on areas with significant thickness losses. For thorough validation, solid finite element models are constructed and subjected to a similar mesh convergence study. The end goal is to demonstrate that the shell finite element model converges and produces realistic stress distributions, providing a robust tool for assessing the tank's structural performance.

4.1 Methodology

The methodology for Phase 2 involves key steps to develop and validate the shell finite element model (FEM) for the tank geometry. A shell mesh model of the tank was created and analysed using ANSYS software to evaluate its structural response under internal pressure.

4.1.1 Shell Mesh Generation

The pre-processed tank remaining wall thickness was imported into ANSYS Workbench, and carbon steel was assigned to the tank wall material within the ANSYS Engineering Data module. A shell meshing element type with quadrilateral elements was selected for flat surfaces. The element size was determined by the geometric complexity of the tank, desired analysis accuracy, and results from a grid independence study. Mesh controls were applied to ensure high-quality mesh across the model, which involved defining minimum and maximum element sizes or setting specific element aspect ratio limitations.

A grid independence study was conducted to establish an appropriate mesh density. This involved creating multiple shell mesh models with varying element sizes and comparing the resulting stress or strain values at critical locations. The mesh demonstrating acceptable convergence of results, with minimal change upon further refinement, was chosen for the final analysis. The final shell mesh model was generated after careful consideration of element type, size, and overall mesh quality, incorporating learnings from the grid independence study. This process ensured that the model would yield converged results with minimal computation time.

4.1.2 Finite Element Analysis Setup

A static structural analysis type was selected to simulate the tank's response to internal pressure. To mimic the filling process, hydrostatic water pressure was applied to the inner surface of the shell mesh model. The pressure distribution was defined as a function of depth, considering water density. A 1000kg/m^3 hydrostatic pressure was used as fluid density and was incorporated to simulate a gradual increase in pressure due to filling.

The bottom face of the tank was fixed with the boundary conditions to represent the tank's support system, ensuring the model is restrained at the base to shows the actual tank's connection to the ground. ANSYS solver settings were chosen based on the analysis type and desired solution convergence criteria. The maximum stress, stress path, total deformation, deformation path and safety of factor, were generated to provide a comprehensive understanding of the tank's structural integrity under various loading conditions.
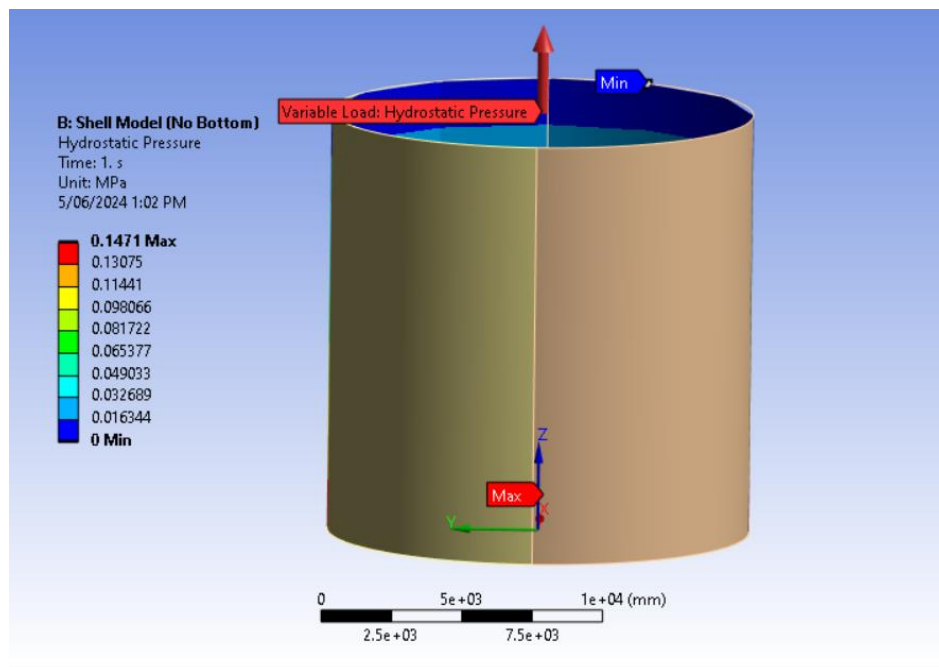
Figure 7:: Boundary conditions and the applied hydrostatic pressure

4.1.3 Data Import into ANSYS

Importing the remaining wall thickness data into Ansys has been challenging due to the nature of the RGB-to-thickness data conversion because of significant errors which occur along the edges of the scan areas. The primary issue arises from how Ansys processes this data, typically using interpolation/spline fitting based on several nearest nodes. While effective for sparse data, this method becomes problematic with dense datasets. Dense data leads to overfitting in the interpolation process, resulting in unrealistic and highly variable thickness values at each node. This localised fitting does not accurately represent the structural integrity of the tank. Instead, averaging the nodal thickness values over areas proportional to the mesh element size is crucial. This approach ensures a more accurate and representative distribution of thickness values, providing a reliable

basis for structural analysis and maintaining the model's integrity and performance. A MATLAB code was created to assist in smoothing the problem. As shown in Figure 8 (a), Close-up of the wall thickness data where errors have occurred at the edges of scan areas.

To address these inconsistencies, a Savitzky-Golay smoothing filter was applied. Designed to act as a moving average over an area encompassing 21x21 data points, this filter smooths the data by averaging the values over a larger area, thereby reducing localised variations. The result, shown in Figure 8(b), demonstrates that the Savitzky-Golay filter effectively reduces the red areas, representing problematic regions in the original data. This smoothing process provides a more consistent and accurate representation of the wall thickness, crucial for reliable analysis and decision-making. All the remaining pictures are in Appendix B.

(a)   (b)
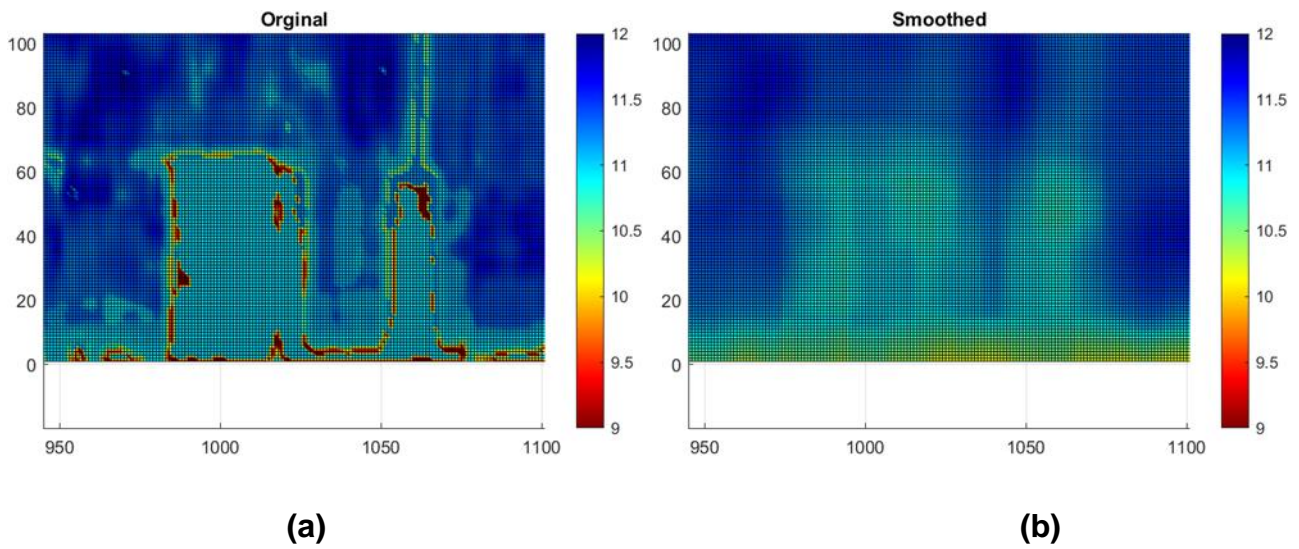
Figure 8: (a) is the Close-up of the wall thickness data where errors have occurred at the edges of scan areas and (b) is the Close-up of the wall thickness data with a moving average filter applied.

(a)   (b)
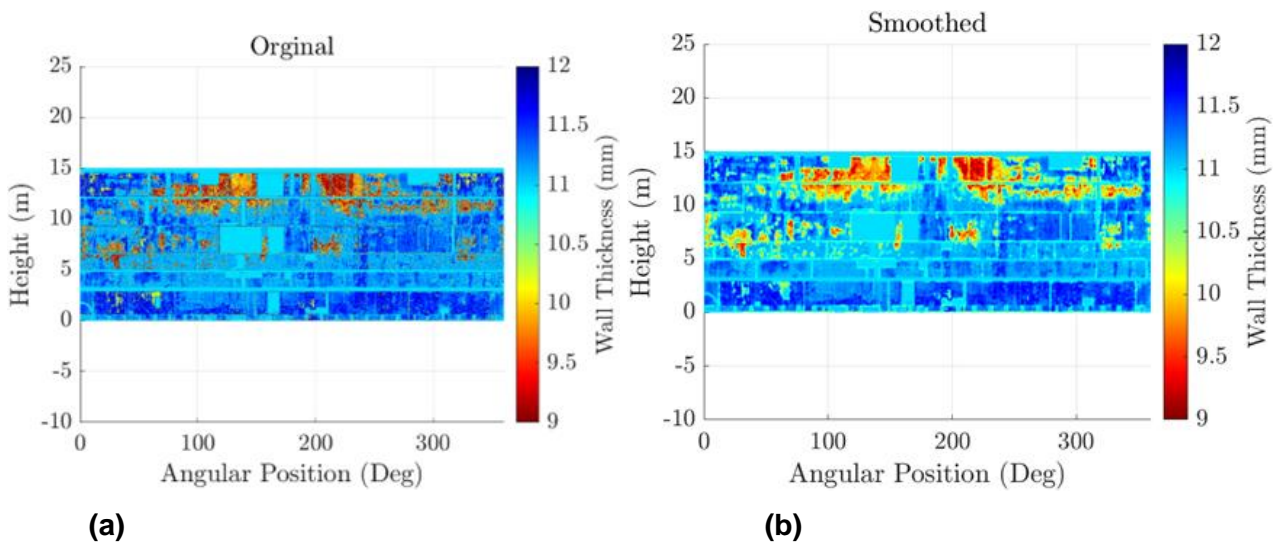
Figure 9: Comparison of wall thickness data (a) without and (b) with a moving average filter applied

The next step involved reducing the data set to match the order of magnitude of the mesh used in Ansys by performing local averaging over areas corresponding to the mesh element size. Figure 9 demonstrates the result, where the data has been averaged to align with the mesh scale. This step is crucial as it ensures that the data used for analysis is consistent with the mesh size, providing more accurate and reliable results. For each mesh size used in a mesh convergence study, a corresponding mesh import dataset was produced. This ensures that the data remains representative and accurate across different mesh scales, allowing for a thorough and precise convergence study. The final step was to reduce the data set to be, of the same order of magnitude as the mesh that will be used in Ansys. This was done by local averaging over the mesh size, see the image Figure 11. The mesh size was produced as this mesh import dataset for each mesh size that was use in mesh convergence study.
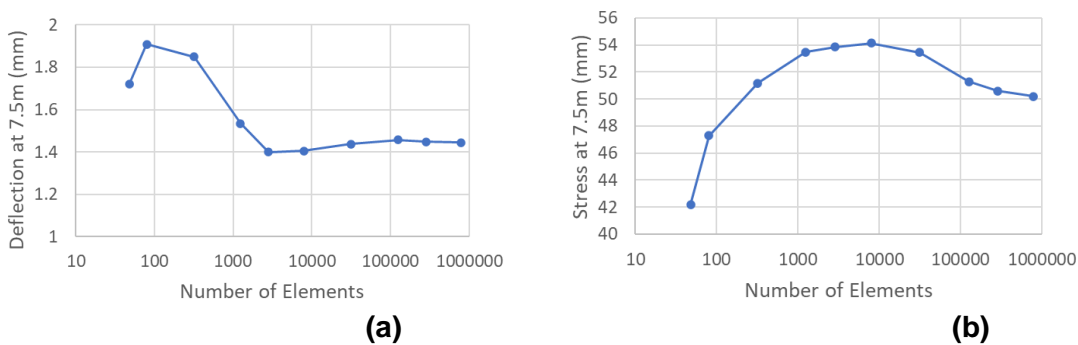
Figure 10: (a) Mesh convergence for deformation and (b) von Mises Stress for the maximum value and at 7.5 m above the base of the tank that intersects the x-axis.

This method enhances the reliability of the structural analysis by maintaining consistency between the data and the mesh used in the simulations. All the remeshed plot at varying scales from 5000mm to 10mm is done and recorded in Appendix B.

Afterward, the data was exported in both Cartesian and Polar coordinates, which were tested in Ansys and performed well. Exporting in these formats provides flexibility in how the data is utilized within Ansys, ensuring compatibility with various modelling approaches, and allowing for a more comprehensive analysis of the tank's structural integrity. This step confirms that the preprocessing and smoothing techniques applied to the remaining thickness loss data are effective and versatile for use in Ansys simulations. The visual presentation is in results 4.2.

4.2 Comparative Analysis Report on Shell Models with and without Imported Thickness Data

Comparing a shell model that incorporates imported thickness data with one that assumes uniform thickness is vital for accurate structural analysis. The model with actual thickness data reflects the true state of the tank, accounting for variations due to wear, corrosion, or manufacturing defects.

This realistic portrayal allows for accurately predicting stress distributions and deformation, identify potential failure points, and make informed decisions regarding maintenance and safety. In contrast, a model without these data might overlook critical weaknesses, leading to underestimations of risk and potentially unsafe conditions. Therefore, the comparison between these two models is essential for ensuring the structural integrity and longevity of tanks in real-world applications.

4.2.1 Result
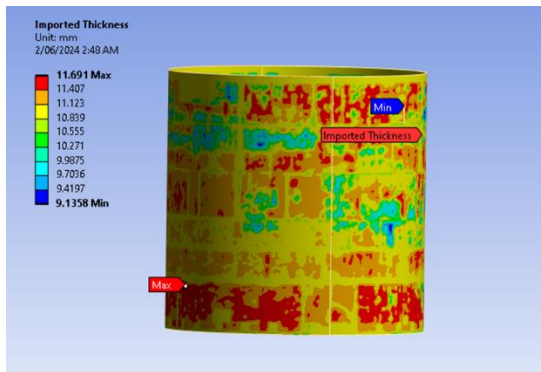
Figure 11: The remaining wall thickness data imported into Ansys
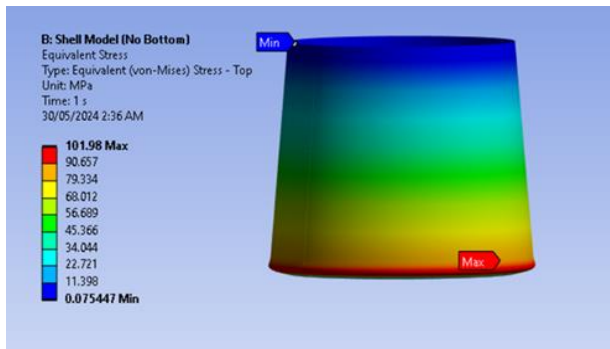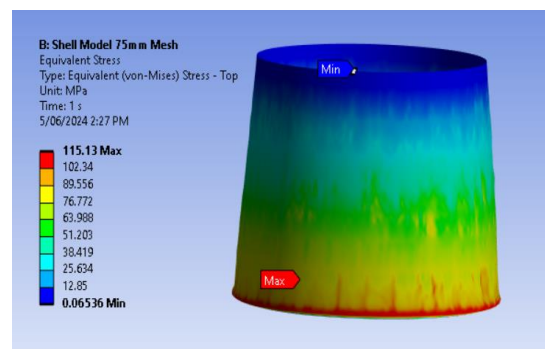
| (a) | (b) |

Figure 12: (a) is the results for the 75 mm mesh shell model with constant 12 mm wall thickness and (b) imported wall thickness geometry
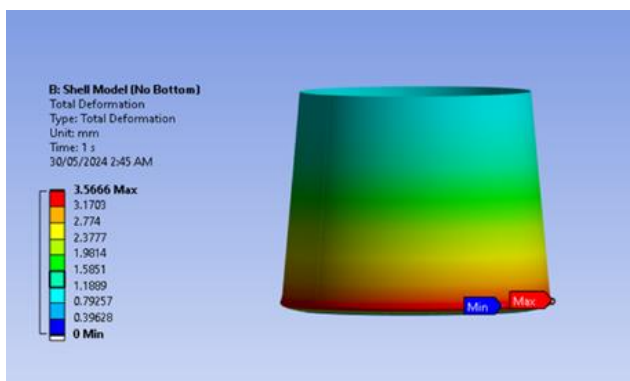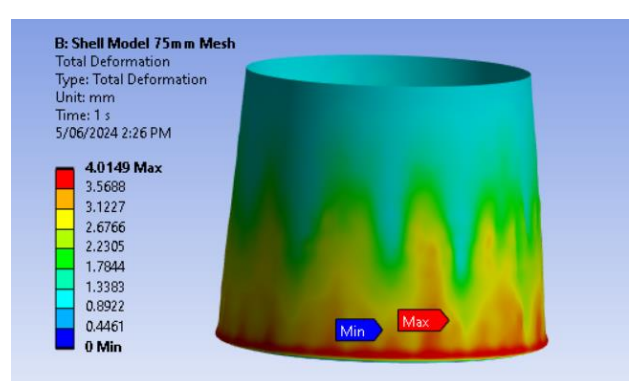
| (b) | (d) |

Figure 13:Result (c) is the deformation for the shell model with constant 12 mm wall thickness and (d) imported wall thickness geometry.

(e)	(f)
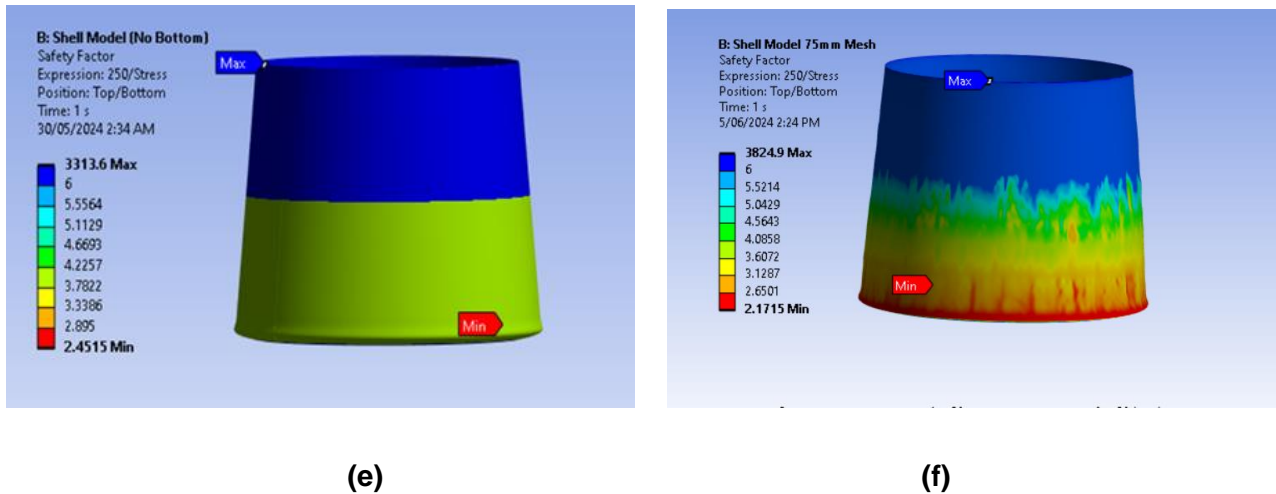
Figure 14:Result (e) is the safety factor for the shell model with constant 12 mm wall thickness and (f) imported wall thickness geometry

4.3   Discussion

4.3.1 Shell model with imported thickness data

The imported thickness data for the tank reveals a range from 9.10 mm to 11.70 mm, highlighting the variability in wall thickness which could significantly influence structural integrity. Subsequent analysis in the shell model shows varying stress levels, with a maximum equivalent stress of 115.10 MPa, which underscores areas potentially at risk under operational loads. Additionally, the total deformation analysis indicates maximum deformation up to 4.01 mm, suggesting some regions are more prone to physical displacement. The corresponding safety factor shows a decrease from 2.44 for the 12 mm nominal wall thickness to 2.17 for the imported thickness geometry. These analyses collectively provide a comprehensive view of the tank's mechanical behaviour and structural health, crucial for maintaining operational safety and integrity.

4.3.2 Shell model without imported thickness data

The "No Bottom" shell model analysis highlights the tank's mechanical properties under simulated conditions. The equivalent stress analysis reveals a maximum stress of 101.98 MPa, identifying areas with high stress concentrations. The total deformation model shows a maximum deformation of 3.56 mm, indicating potential structural integrity and operational safety concerns. The safety factor analysis, with a minimum value of 2.45, suggests that while the structure remains within safety thresholds (American Petroleum Institute 2001), certain regions may require further scrutiny or reinforcement. This analysis is crucial for evaluating the tank's resilience, guiding maintenance, and ensuring long-term functionality. The "No Bottom" shell model was specifically simulated to isolate and examine the mechanical behaviour of the tank's walls, focusing on stress concentrations and

deformation without the influence of the bottom structure. Although bottomless tanks are not used in practice, this theoretical model provides valuable insights into stress distribution and structural resilience in the tank's vertical walls.

4.3.2 The comparison between the two models of the tank.

The comparison between the two models of the tank, reveals distinct differences in their structural responses under similar conditions. In the model without the bottom, the maximum equivalent stress observed is significantly higher, indicating increased stress concentrations that could potentially compromise the tank's structural integrity. In contrast, the total deformation is slightly lower in the model without the bottom, suggesting that removing the bottom portion may somewhat reduce the overall deformation under load, possibly due to reduced constraints that allow for more uniform stress distribution. However, the safety factor analysis for both models shows a decrease when the bottom is removed, with the minimum safety factor values approaching lower safety thresholds. This could indicate that the absence of the bottom makes the structure more susceptible to failure under certain conditions, emphasising the importance of the bottom segment in providing structural stability and distributing loads more effectively. Overall, the bottomless model, while showing less deformation, presents higher stress concentrations and reduced safety margins, highlighting its increased vulnerability compared to the complete model.

4.3 Solid Mesh (introduced in this phase)

The thickness measure of 12mm for the tank geometry was used in ANSYS Workbench. Identical material properties were assigned to ensure consistency between shell and solid models. A solid mesh was generated using the same analysis setup as the shell model was followed, including static structural analysis and hydrostatic pressure application. Identical boundary conditions and ramped pressure loads were applied. The model was solved, and plots for stress, total deformation, and safety of factor were generated with all the paths analysed.

4.4 Analytical models (introduced in this phase)

This section focuses on analytical calculations to evaluate the structural integrity of the tank shell, especially in areas affected by corrosion. Analytical models validate finite element model (FEM) results and ensure compliance with industry standards. Using standardised procedures for thickness measurement and minimum thickness calculation, this section aims to establish a benchmark for assessing the tank's suitability for service.

4.5 Eigenvalue Buckling Analysis Setup

The Eigenvalue Buckling Analysis Setup involves three main steps. The first step is Pre-Stress Application, where pre-stress conditions (Static Structural) are applied to simulate realistic operational conditions. The second step, Analysis Settings Configuration, configures the settings to

perform an eigenvalue buckling analysis, crucial for understanding the tank's buckling behaviour under various loads. The third step, Solution Evaluation, reviews solution results, including total deformation outputs for multiple modes (Total Deformation 1 through 10), essential for identifying potential buckling modes and assessing the tank's structural stability. By following these steps, a well-defined shell mesh model and analysis setup were established in ANSYS, preparing the model for further evaluation in subsequent phases.

4.6 Results

4.6.1 Solid Model
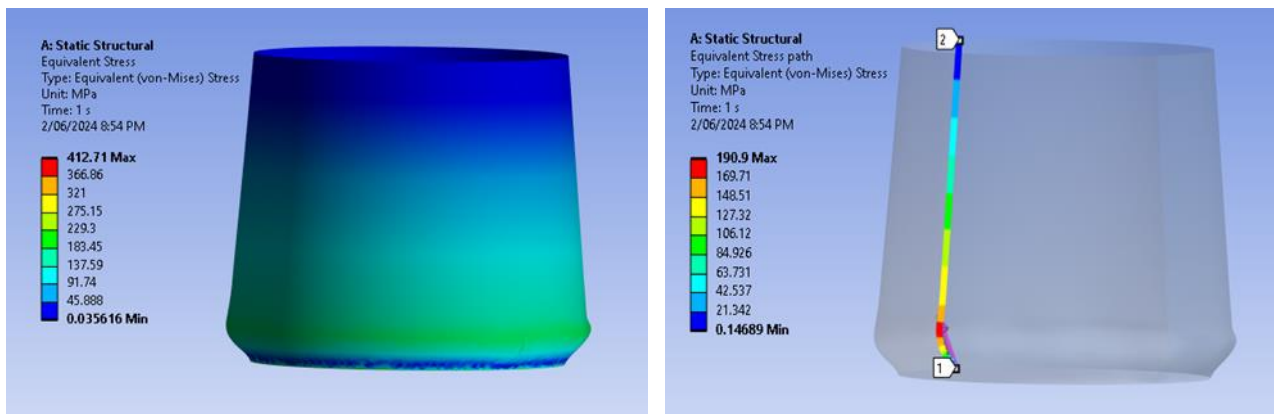
(a)   **(b)**

Figure 15: Results for von mises stress (a) and the path (b) for solid model
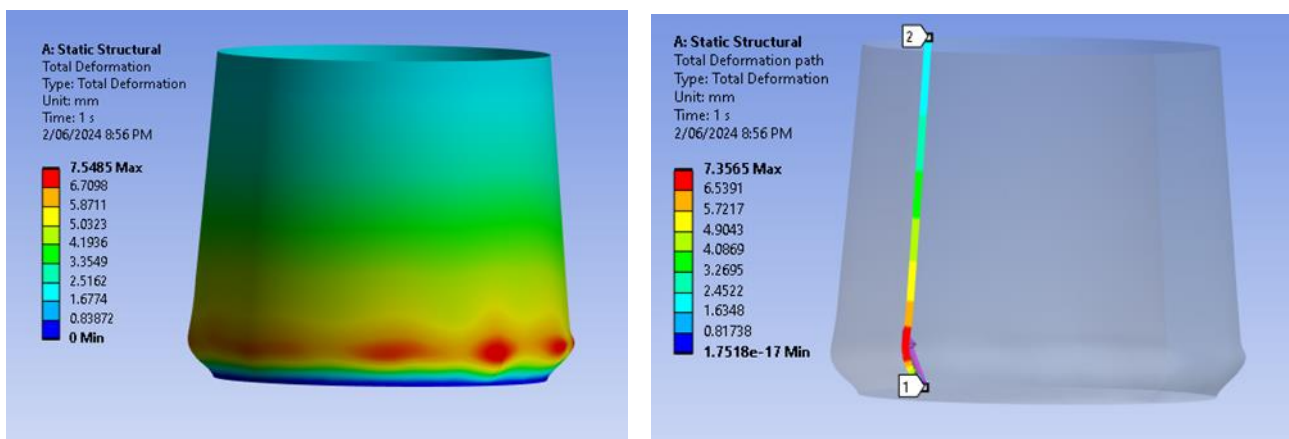
(c)   **(d)**

Figure 16: Result for the total deformation (c) and the path (d) for the solid model.
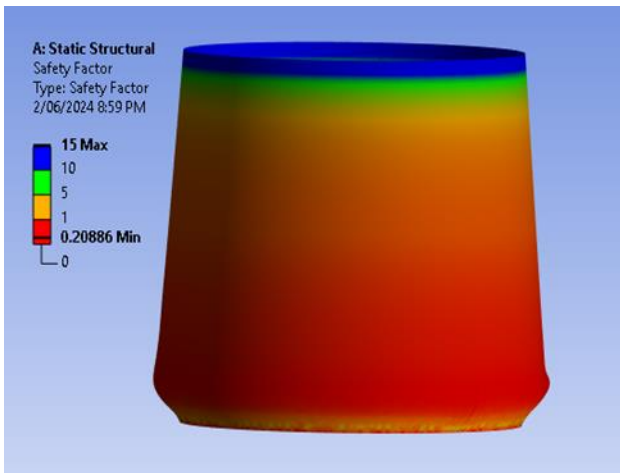
(e)
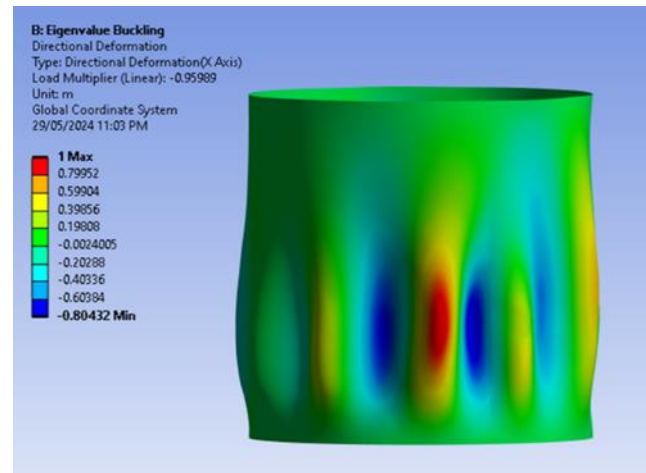
(f)

Figure 17: Result for safety factor (e) and the total buckling deformation (f).

4.7 Discussion and summary

The analysis using static structural simulations provides critical insights into the tank's structural integrity. Equivalent stress data indicate that the maximum stress experienced by the tank is 412.71 MPa, which occurs at the base, progressively decreasing towards the top. The path of stress along the height shows a peak stress of 190.9 MPa. Total deformation results show a maximum deformation of 7.5485 mm, occurring at the lower regions of the tank, demonstrating that these areas experience the most significant displacement under load. A deformation path analysis confirms these results, indicating maximum deformation along the bottom edge, emphasizing the need for focused structural reinforcement in these areas. Additionally, the safety factor analysis reveals a minimum value of 0.20886, which is critical as it falls below typical industry standards for safety, necessitating a review of material choice or design parameters to enhance the tank's safety and operational reliability.

6.THE FEA MODELS COMPARED TO THE EVALUATION OF THE STANDARD.

The analysis of tank integrity using analytical calculations provides a good foundation for evaluating the structure's safety and compliance with industry standards. This phase focuses on employing empirical formulas from the API 653 standard (American Petroleum Institute 2001) to calculate safety factors to compare results from finite element analysis. By correlating these analytical calculations with practical data from material properties and design stress limits, such as those of ASTM A283-C steel, the evaluation aims to confirm that the tank's structure meets the requisite safety thresholds for both lower and upper courses (American Petroleum Institute 2001). To evaluate what the standard considers a satisfactory safety factor using the table 1 below, has a list of yield, tensile and allowable product stresses. It is best to assume that steel has the worst properties, like A 283-C. Based on the allowable produced stress, there will be a safety factor for the lower two strakes and another for the upper strakes.

Table 1:Maximum allowable stresses for factor of safety calculations/ other factors.

Table 4-1 Maximum Allowable Shell Stresses
(Not For Use For Reconstructed Tanks, see Note 6)

Material Specification and Grade	Minimum Specified Yield Stress, Y (lbf/in.^{2})	Minimum Specified Tensile Strength, $\square$ T(lbf/in.^{2})	Allowable Product Stress, S (lbf/in.^{2}) (7)	
			Lower Two Courses	Upper Courses
ASTM Specifications				
A 283-C	30,000	55,000	23,600	26,000

Calculating the safety of factor,

To evaluate what the standard considers a satisfactory safety factor, Table 4-1 of the API standard was used, which has a list of yield, tensile and allowable product stresses for the bottom two and upper strakes. In this analysis, the steel with the worst material properties was used, similar to A 283-C. Based on the allowable produced stress for this material, the safety factor for the bottom two strakes and upper strakes is 1.27 and 1.16, respectively. In addition, the effective stress (in lbf/in2) in each strake is estimated in the API standard as

$$S = \frac{2.6\,HDG}{tE}$$

where H is the height from the bottom of the strake to the height of the maximum liquid level (in ft), D is the diameter of the tank (in ft), G is the highest specific gravity of the contents (assumed 1.3 for

20

this analysis) and E the weld joint efficiency of the tank (assumed equal to 1 for this analysis). t is the minimum effective wall thickness for a scan area.
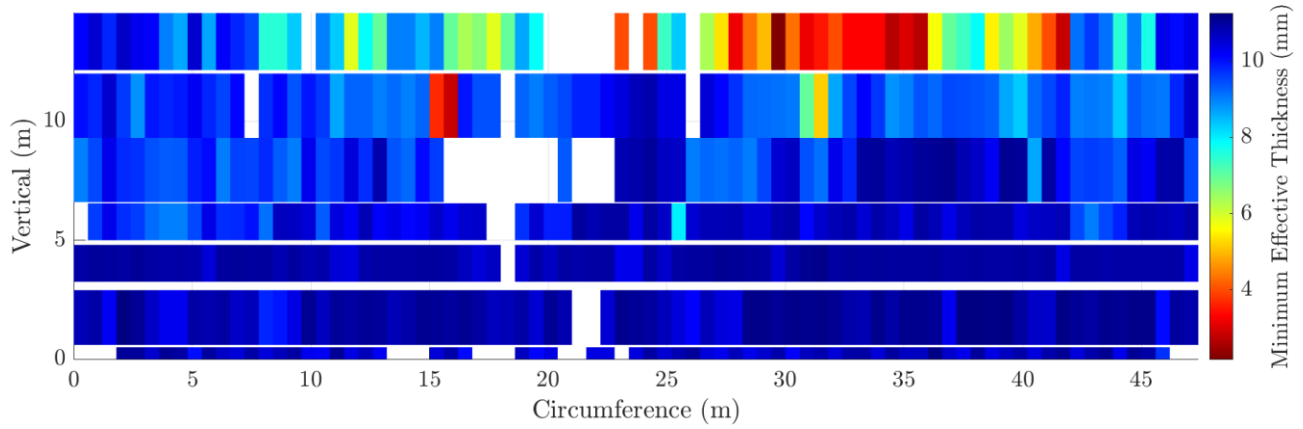
Figure 18:The minimum effective wall thickness (t) for the various scan areas.
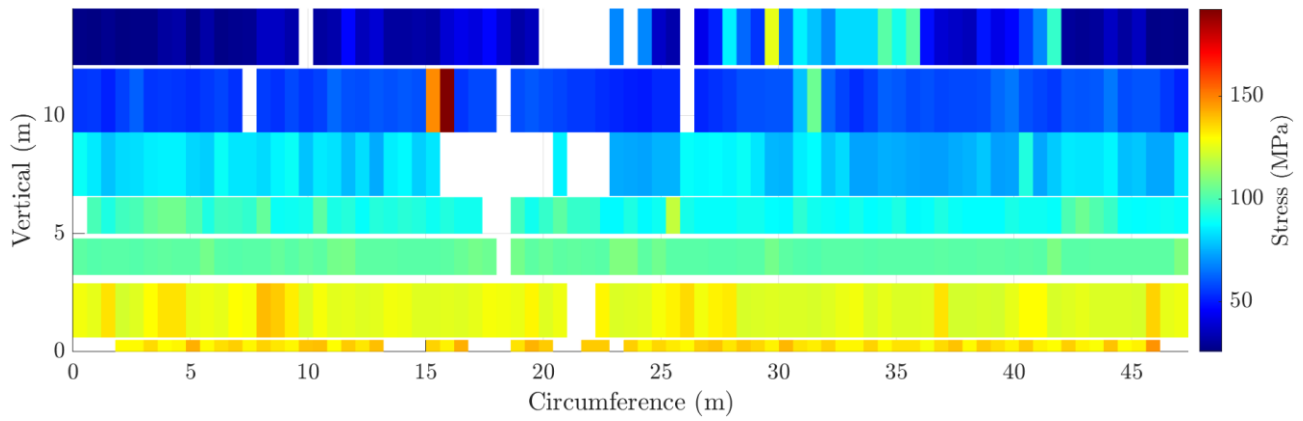
Figure 19:The minimum effective stress (S) for the various scan areas
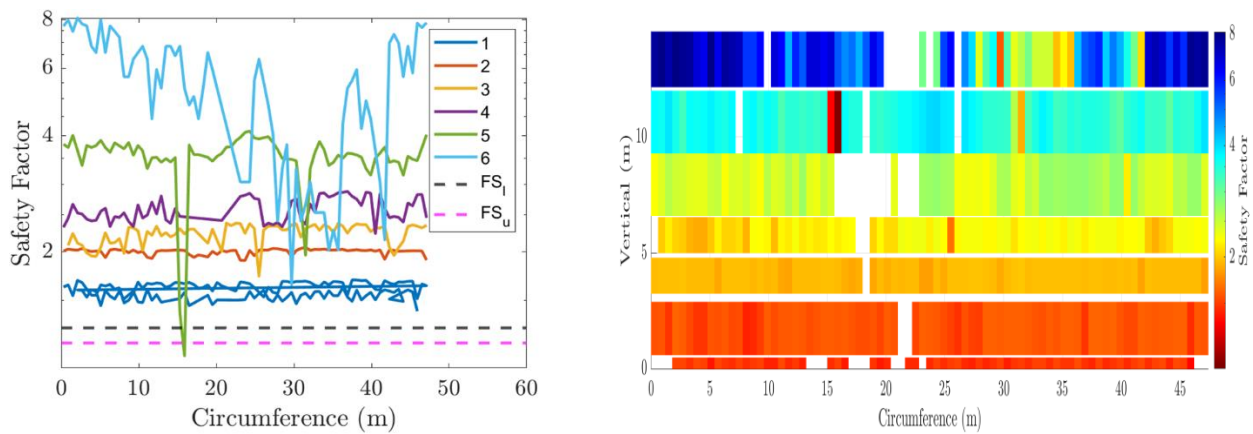
Figure 20:The plot of the safety factor for each strake against the circumference and compared to the minimum safety factor for the lower two (FS$_l$) and upper (FS$_u$) strakes.
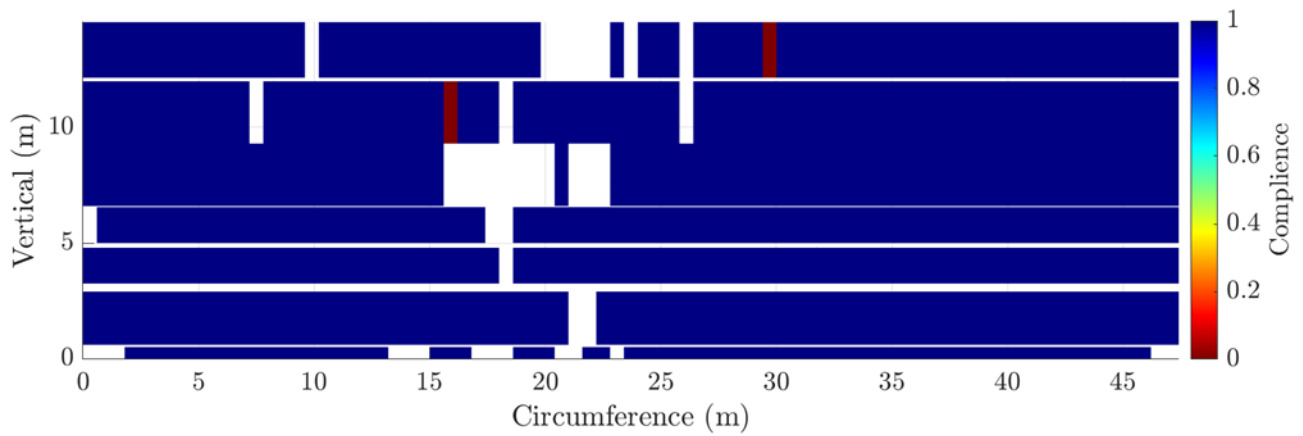
Figure 21:Compliance Analysis.

A compliance analysis is performed, to check the safety factor to ensure its not exceeded, and the minimum wall thickness is not less than 2.54 mm, as required by the API 653 standard. In the compliance analysis, two zones were identified as non-compliant. The first issue is in the 5th strake, where the safety factor does not meet the required standards. The second issue arises in the 6th strake, where the wall thickness falls below the minimum allowable threshold.

6.1 Safety of Factor

Safety Factor analysis, using ANSYS for finite element modelling, integrates real-world conditions such as material yield stress, efficiency of welded joints, and the hydrostatic pressure is used as a fluid, to generate a detailed stress profile across the tank. The models help visualise areas of potential weakness where the safety factor is below the acceptable threshold. For instance, the visual representations from ANSYS clearly show regions where the SF dips dangerously low, indicating critical zones that requires some structural reinforcement or operational adjustments such as reducing the fill level.

By emphasising the Safety Factor in the analysis, the model aligns more closely with industry standards that prioritise not just compliance with maximum fill heights but also ensuring a safety buffer. This approach not only helps in pinpointing specific structural weaknesses but also in validating the effectiveness of the design under maximum operational loads. Consequently, Safety Factor provides a more comprehensive understanding of the tank's safety and durability, making it an essential aspect of the structural assessment and design optimisation process.

7. CONCLUSION

This project highlights the successful development of a methodology to utilise phased array ultrasonic thickness (PAUT) data for creating a shell finite element model (FEM) to evaluate the stresses and structural integrity of steel surface tanks. This methodology was achieved through a phased approach that addressed each objective of the project.

Firstly, the data collection and processing phase involved gathering essential data from industry partners, which was then processed using MATLAB. This phase was crucial for creating accurate representations of tank wall loss, which are vital for the subsequent modelling and analysis steps. The use of MATLAB allowed for precise data manipulation and visualisation, ensuring a great foundation for the finite element analysis.

In the development phase, both shell and solid finite element models were created using ANSYS. The shell model demonstrated significant computational efficiency, making it suitable for preliminary assessments. In contrast, the solid model provided detailed insights into stress and strain distributions, particularly in areas with significant thickness variations. Both models underwent various validation through a convergence study and comparison with industry standards, ensuring their reliability and accuracy.

The comparison and validation phase focused on assessing the accuracy of the shell FEM by comparing it against the solid FEM. The results indicated that while the shell model is effective for initial evaluations due to its computational efficiency, the solid model offers detailed and precise insights, especially in regions with complex stress distributions. This comparison affirmed that the methodology developed could reliably assess the structural integrity of steel tanks, meeting or exceeding the minimum safety factors specified by empirical standards.

During the compliance assessment phase, a compliance map was created to highlight areas of non-compliance, particularly in the 5th and 6th strokes. These findings underscored the importance of reinforcement and optimisation to ensure the safety and efficiency of the tanks. Addressing these non-compliant areas is crucial for maintaining the structural integrity of the tanks and preventing potential failures.

In conclusion, this project successfully achieved its objectives by integrating PAUT data with FEM to enhance the structural integrity assessment of steel tanks. The methodology developed provides a reliable and efficient tool for evaluating the condition of storage tanks, contributing to safer and more effective maintenance strategies. Future research should focus on refining these models and integrating advanced signal processing algorithms to further improve the accuracy of corrosion assessments. This will ensure the continued reliability and safety of steel storage tanks, supporting the broader goals of industrial safety and environmental protection.

7.1 FUTURE RESEARCH DIRECTIONS

Future research should focus on enhancing the PAUT corrosion mapping equipment and developing high-frequency ultrasonic transducers for early detection of pitting corrosion. The integration of advanced signal processing algorithms and artificial intelligence could improve the reliability of corrosion assessments (Khalaf et al., 2024). A shift towards hybrid modelling approaches that leverage the strengths of both shell and solid finite element models is necessary. This could enhance the predictive accuracy of structural integrity assessments (Sarwar et al., 2024). Additionally, future research should aim to develop protocols and software solutions that facilitate the integration of ultrasonic testing data into FEA software, ensuring accurate reflection of actual corrosion patterns in steel tanks (Olisa et al., 2021).

Comprehensive models incorporating electrochemical corrosion mechanisms at the microscale with structural stress analyses at the macroscale could offer insights into the progression of corrosion over time. To ensure the reliability of advanced methodologies, comprehensive validation studies comparing predictions against actual case studies of steel tanks subjected to corrosion are imperative.

The application of these advanced models to evaluate the structural integrity of tanks, examining stress distribution and potential failure modes, should be investigated. Future studies focusing on these research directions can enhance the accuracy and reliability of structural integrity evaluations, leading to safer maintenance of tank structures.

BIBLIOGRAPHY

American Petroleum Institute (2001). API Standard 653, tank inspection, repair, alteration, and reconstruction (3rd Ed.). API Publishing Services.

Ali Hussein Khalaf, Xiao, Y., Xu, N., Wu, B., Li, H., Lin, B., Nie, Z., & Tang, J. (2024). Emerging AI Technologies for Corrosion Monitoring in Oil and Gas industry: A Comprehensive Review. *Engineering Failure Analysis*, *155*, 107735–107735. https://doi.org/10.1016/j.engfailanal.2023.107735

Hassani, S., & Dackermann, U. (2023). A Systematic Review of Advanced Sensor Technologies for Non-Destructive Testing and Structural Health Monitoring. *Sensors*, *23*(4), 2204–2204. https://doi.org/10.3390/s23042204

Ilman, E. C., Wang, Y., Wharton, J. A., & Sobey, A. J. (2020). The impact of corrosion-stress interactions on the topological features and ultimate strength of large-scale steel structures. *Thin-Walled Structures*, *157*, 107104–107104. https://doi.org/10.1016/j.tws.2020.107104

Masserey, B., Raemy, C., & Fromme, P. (2014). High frequency guided ultrasonic waves for hidden defect detection in multi-layered aircraft structures. *Ultrasonics*, *54*(7), 1720–1728. https://doi.org/10.1016/j.ultras.2014.04.023

Nakai, T., Matsushita, H., & Yamamoto, N. (2006). Effect of pitting corrosion on strength of web plates subjected to patch loading. *Thin-Walled Structures*, *44*(1), 10–19. https://doi.org/10.1016/j.tws.2005.09.004

Ojha, M., & Dhiman, A. (2010). Problem, Failure and Safety Analysis of Ammonia Plant: a Review. *International Review of Chemical Engineering (I.RE.CH.E.)*, *2*(6). https://citeseerx.ist.psu.edu/document?repid=rep1&type=pdf&doi=044721bc3712806a5679abfe0a8414b1c4efff6a

Sarwar, U., Ainul Akmar Mokhtar, Muhammad, M., Rano Khan Wassan, Afzal Ahmed Soomro, Majid Ali Wassan, & Shuaib Kaka. (2024). Enhancing pipeline integrity: a comprehensive review of deep learning-enabled finite element analysis for stress corrosion cracking prediction. *Engineering Applications of Computational Fluid Mechanics*, *18*(1). https://doi.org/10.1080/19942060.2024.2302906

Silva, J. E., Garbatov, Y., & Guedes Soares, C. (2013). Ultimate strength assessment of rectangular steel plates subjected to a random localised corrosion degradation. *Engineering Structures*, *52*, 295–305. https://doi.org/10.1016/j.engstruct.2013.02.013

Smith, (2018). *The impact of corrosion on the structural integrity of steel storage tanks. international journal of corrosion and control, 45(2), 123-135.* (Jones, M, Ed.).

Sultana, S., Wang, Y., Sobey, A. J., Wharton, J. A., & Shenoi, R. A. (2015). Influence of corrosion on the ultimate compressive strength of steel plates and stiffened panels. *Thin-Walled Structures*, *96*, 95–104. https://doi.org/10.1016/j.tws.2015.08.006

Thakur, A., & Kumar, A. (2021). Sustainable Inhibitors for Corrosion Mitigation in Aggressive Corrosive Media: A Comprehensive Study. *Journal of Bio- and Tribo-Corrosion*, *7*(2). https://doi.org/10.1007/s40735-021-00501-y

Wang, R. (2021). On the effect of pit shape on pitted plates, Part II: Compressive behavior due to random pitting corrosion. *Ocean Engineering*, *236*, 108737. https://doi.org/10.1016/j.oceaneng.2021.108737

Zhang, Y., Huang, Y., & Yong Sen Wei. (2017). Ultimate strength experiment of hull structural plate with pitting corrosion damage under unaxial compression. *Ocean Engineering*, *130*, 103–114. https://doi.org/10.1016/j.oceaneng.2016.11.065

Zhao, Z., Dai, B., Xu, H., & Li, T. (2021). Bending capacity of corroded welded hollow spherical joints with considering interaction of tension force and bending moment. *Structures (Oxford)*, *34*, 2656–2664. https://doi.org/10.1016/j.istruc.2021.09.042

Zhu, H., Chen, J., Lin, Y., Guo, J., Gao, X., Chen, Y., Ge, Y., & Wang, W. (2024). In-Line Inspection (ILI) Techniques for Subsea Pipelines: State-of-the-Art. *Journal of Marine Science and Engineering*, *12*(3), 417. https://doi.org/10.3390/jmse12030417

APPENDICES

Appendix A: Phase 1 Data processing and standard evaluation
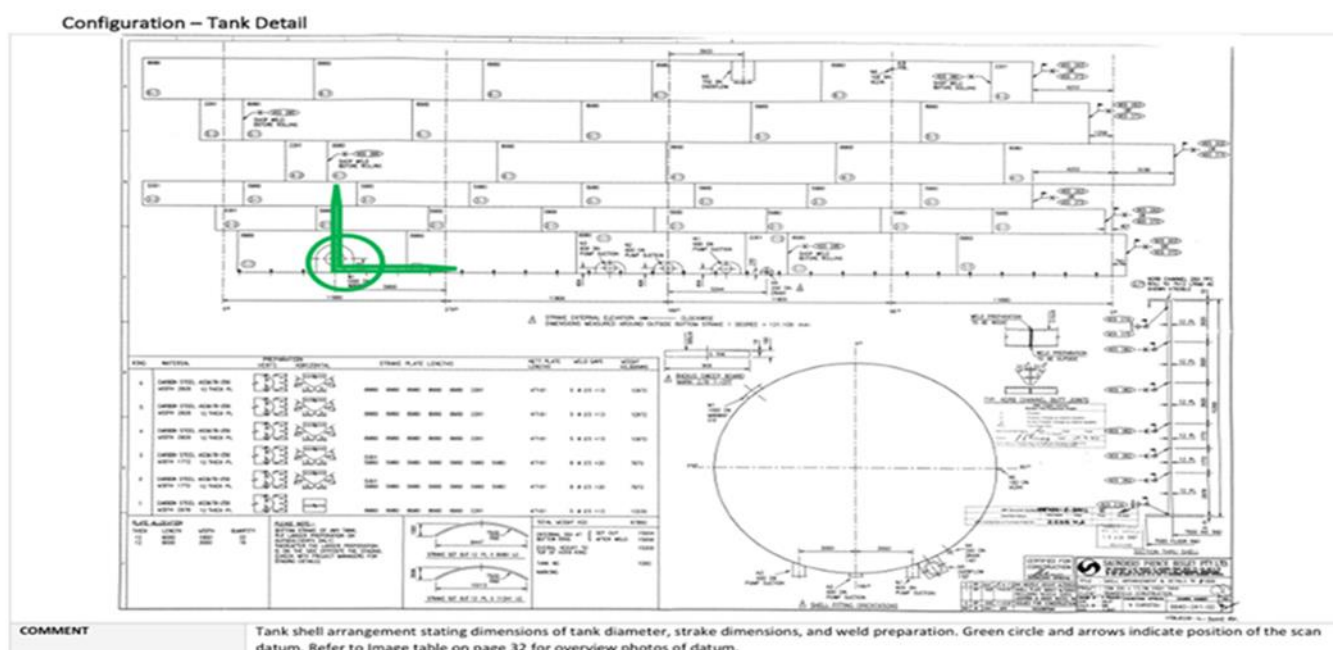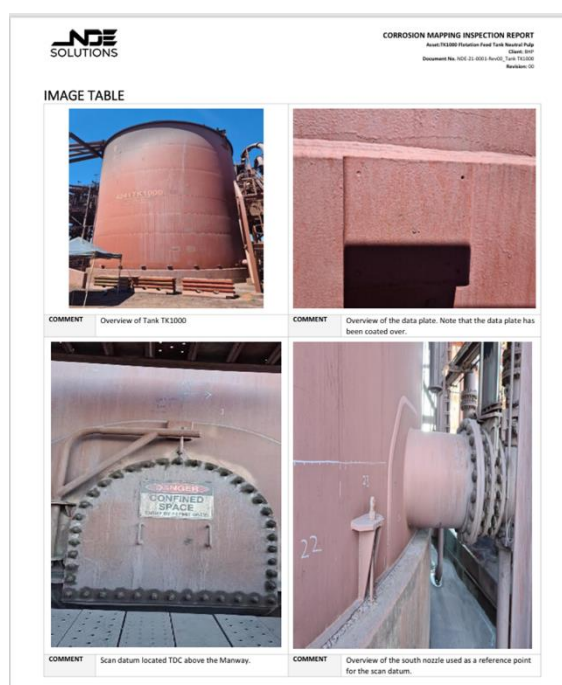

Figure 22:Tank geometry.

Figure 23:The overview of the tank showing the location in which all the data are taken.

Appendix B: Phase 2: Shell Modelling and Mesh validation

The series of heat maps visualises results from a detailed remeshing study on ultrasonic thickness measurement data of a tank, crucial for assessing structural integrity by evaluating wall thickness variations.

Initial Data Analysis:

The first set of images compares original thickness data against its smoothed counterpart at a 10mm mesh. The original data, characterised by significant noise and variability due to measurement techniques or actual structural issues such as corrosion, contrasts with the smoothed data. The smoothing process reduces noise, highlighting true areas of concern and providing a clearer picture of potential material compromise.

Progressive Remeshing:

Subsequent images display the data remeshed at resolutions from coarse (5000mm) to very fine (10mm). Coarser meshes (5000mm to 1500mm) generalise the tank's wall thickness, suitable for broad overviews and initial assessments to identify large-scale degradation or defects. As mesh size decreases (750mm to 150mm), increased resolution allows identification of smaller defects like minor corrosion spots or uneven thickness. The finest meshes (75mm to 10mm) offer a high-resolution view of the tank's structure, critical for pinpointing exact locations of potential structural failure and for detailed engineering analysis.

Applications and Insights:

These visualisations are vital for assessing the tank's current state. Areas with significant thinning or anomalies are prioritised for repairs or closer monitoring, enhancing safety and operational reliability. The progression from original to smoothed and various remeshed data verifies the accuracy of thickness measurements. For simulation of the tank's behaviour under stress, these maps provide essential calibration data to ensure model accuracy.

Overall, the comprehensive data represented in these heat maps aids in making informed decisions about the data to be imported into assist for further analysis.
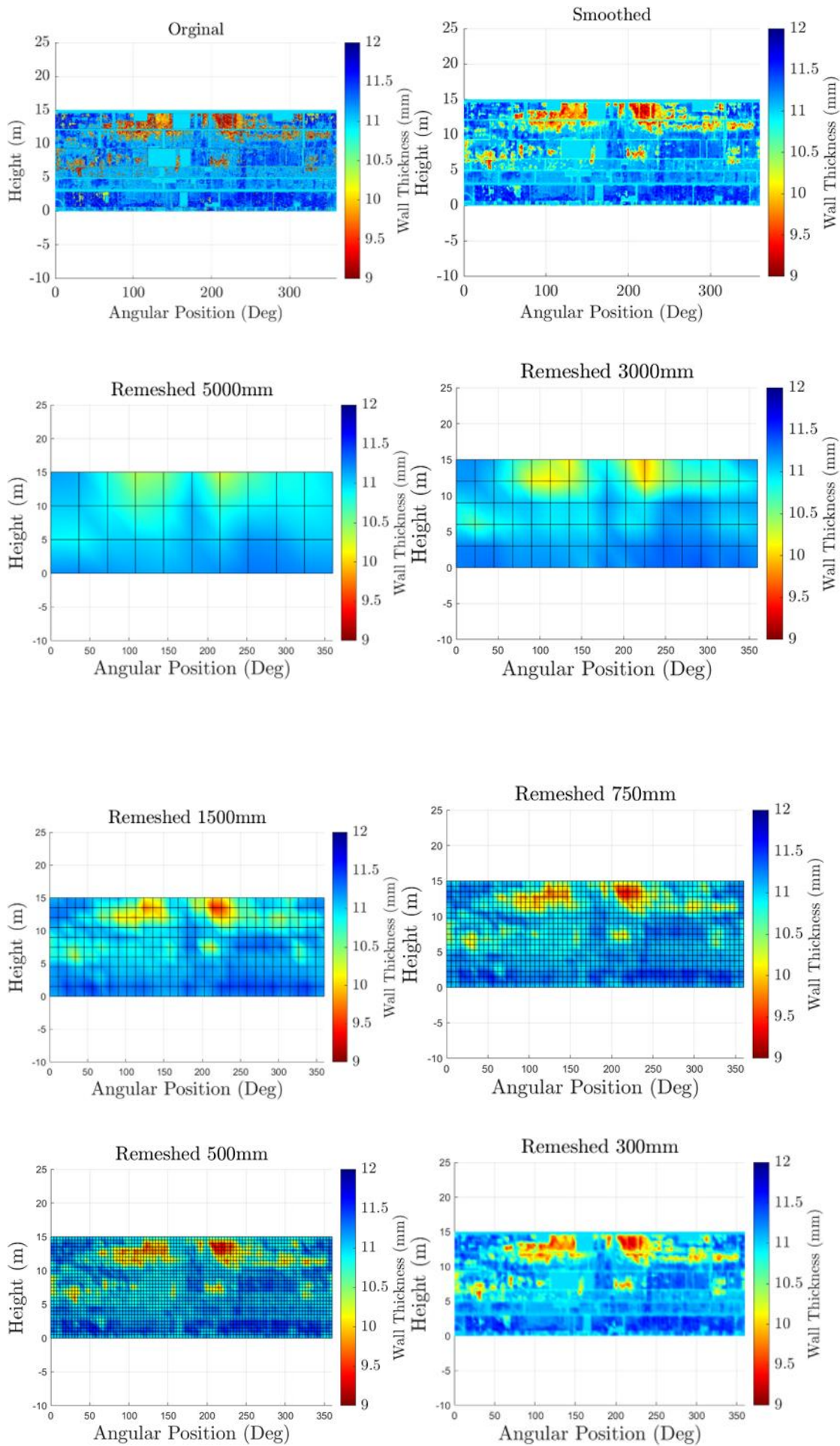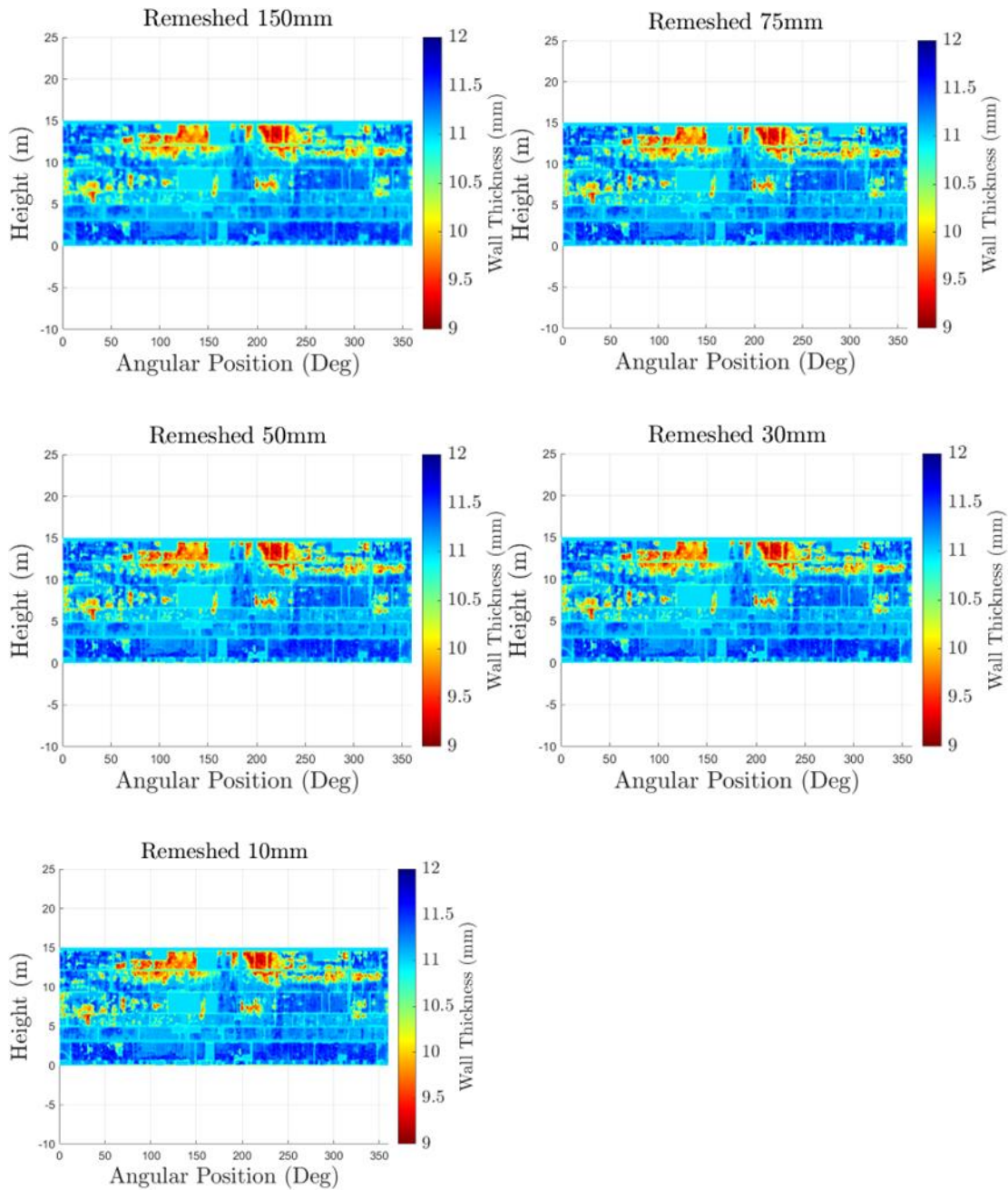
After remeshing, the data was imported into ANSYS for shell model analysis, allowing for a refined evaluation of the tank's structural integrity. This step involved integrating the remeshed data into ANSYS, applying relevant material properties and boundary conditions, and conducting simulations to assess stress distribution and potential weak points under operational conditions. The results from this analysis help identify areas requiring reinforcement/closer monitoring, ensuring the model accuracy.

The analysis of the FEM model with the imported data, Mesh convergence study.

Table 2:The independence convergence study for shell model.

Mesh Size (mm)	Number Nodes	Number Elements	Deformation @ Max (mm)	Deformation @ 7.5m (mm)	Stress @ Max (MPa)	Stress @ 7.5m (MPa)
5000	70	48	3.7162	1.7203	99.253	42.21
3000	96	80	3.9137	1.9082	104.16	47.305
1500	352	320	4.2799	1.8484	114.7	51.184
750	1302	1240	4.3453	1.5354	118.7	53.472
500	2914	2820	4.1079	1.3997	114.84	53.86
300	8058	7900	4.2024	1.4057	116.34	54.129
150	31714	31400	4.0172	1.4367	114.86	53.447
75	126228	125600	4.0149	1.4568	115.13	51.29
50	283542	282600	4.0052	1.448	115.68	50.593
30	786570	785000	4.0038	1.4449	116.45	50.185

Table 3:Percent difference from 30mm mesh values

Mesh Size (mm)	Number Nodes	Number Elements	% Difference Deflect @ Max (mm)	% Difference Deflect @ 7.5m (mm)	% Difference Stress @ Max (Mpa)	% Difference Stress @ 7.5m (Mpa)
5000	70	48	7.18%	19.06%	14.77%	15.89%
3000	96	80	2.25%	32.06%	10.55%	5.74%
1500	352	320	6.90%	27.93%	1.50%	1.99%
750	1302	1240	8.53%	6.26%	1.93%	6.55%
500	2914	2820	2.60%	3.13%	1.38%	7.32%
300	8058	7900	4.96%	2.71%	0.09%	7.86%
150	31714	31400	0.33%	0.57%	1.37%	6.50%
75	126228	125600	0.28%	0.82%	1.13%	2.20%
50	283542	282600	0.03%	0.21%	0.66%	0.81%
30	786570	785000	0.00%	0.00%	0.00%	0.00%

Deformation @ Max and @ 7.5 m: These graphs should show deflection values stabilising as the mesh size decreases. If deflection values level off, that indicates convergence.

Stress @ Max and @ 7.5 m: Like deflection, these graphs should show stress values becoming consistent as the mesh size gets smaller. A plateau or minimal change in stress values with decreasing mesh size is a good indicator of convergence.
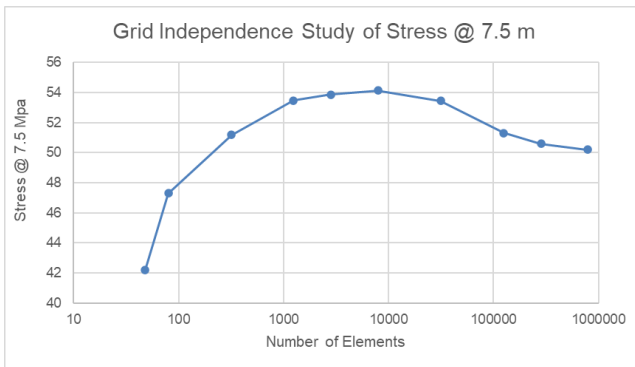
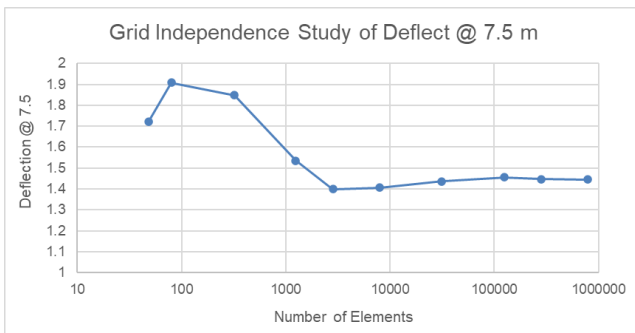**Figure 24:The grid independence study at stress 7.5m**

Figure 25:The grid independence study at deflection at 7.5m

The convergence study displayed in the charts is an integral part of validating the finite element model (FEM) of the tank. This study aims to identify the mesh size that ensures accurate and reliable stress and deformation predictions without excessive computational cost.

In the provided results, various mesh sizes from 5000 mm down to 30 mm were tested for their effects on the maximum deflection and stress at different tank heights (at the maximum stress/deflection points and at a 7.5 m height from the base). The number of nodes and elements increases significantly as the mesh size decreases, which typically improves the precision of the FEM results but requires more computational resources.

Key Observations from the Study:

- **Deformation and Stress Trends:** The data shows that as the mesh becomes finer, the recorded deflection and stress values tend to stabilise. This trend is visualised in the line graphs, where the plotted points start to level off as the mesh size decreases, indicating lesser variability in the results with smaller mesh sizes.

- **Convergence Point:** Convergence seems to occur around the 75 mm mesh size. At this mesh refinement, the percentage difference in both deflection and stress values relative to the 30 mm mesh (the finest mesh tested) falls within 2%. Specifically, the maximum deflection at the 75 mm mesh size shows a difference of only 0.28% compared to the 30 mm mesh, and the maximum stress shows a 1.13% difference.

- **Percent Differences:** The table underscores that larger mesh sizes (5000 mm to 300 mm) exhibit higher percent differences from the 30 mm mesh, confirming less accuracy in the simulation results. These differences decrease markedly as the mesh is refined.

Conclusion of the Study:

The convergence at a 75 mm mesh size suggests that this granularity offers a practical balance between computational efficiency and model accuracy. Using a 75 mm mesh is sufficient to capture critical stress and deflection behaviours of the tank under simulated conditions, providing confidence in the structural analysis and design recommendations based on this model. Thus, it is an optimal choice for further analyses, ensuring detailed insight into the structural integrity of the tank while managing simulation time and resource use effectively.

APPENDIX C: ANALYSIS AND COMPARISON OF THE FINITE ELEMENT.

Table 4:The independence convergence study for solid model.

Mesh Size (mm)	Number of Nodes	Number of Elements	mm		Mpa	
			Deformation @ Max	Deformation @ 7.5m	Stress @ Max	Stress @ 7.5m
500	57376	28226	5.4124	3.0777	167.43	84.77
300	88900	46879	6.204	3.8739	407.93	76.289
200	218139	107687	7.3565	3.9988	190.9	92.23
150	621270	308281	7.6804	3.7133	186.45	92.806
100	811921	405024	8.1059	3.9665	182.99	92.373

The percentage difference for each metric when compared to the smallest mesh size (100 mm mesh size) for the given data.

Table 5:Percent difference from 100mm mesh values

Mesh Size	Number of Nodes	Number of Elements	Deflect @ Max (%)	Deflect @ 7.5 (%)	Stress @ Max (%)	Stress @ 7.5 (%)
500	57376	28226	-33.38%	-22.42%	-8.68%	-8.24%
300	88900	46879	-23.46%	-2.33%	+122.97%	-17.40%
200	218139	107687	-9.25%	+0.81%	+4.32%	-0.15%
150	621270	308281	-5.25%	-6.38%	+1.89%	+0.47%
100	811921	405024	0.00%	0.00%	0.00%	0.00%

Results of the convergence study.

The mesh sensitivity analysis for the tank model emphasises the impact of mesh refinement on computational results, focusing on deformation and stress at various mesh sizes. As the mesh size reduces from 500 mm to 100 mm, the number of nodes and elements consistently increases, enhancing model fidelity. At 500 mm, the model has 57,376 nodes and 28,226 elements, while at 100 mm, it increases significantly to 811,921 nodes and 405,024 elements, indicating a more detailed model. For deformation, maximum deflection percentage decreases substantially as the mesh refines, from -33.38% at 500 mm to 0.00% at 100 mm, the baseline. The deflection at 7.5% load condition also varies considerably, initially decreasing from -22.42% to +0.81% at 200 mm, then returning to zero at the finest mesh. This suggests coarser meshes might overestimate deformations, resulting in less accurate simulations.

Stress analysis reveals a more complex behaviour. At 500 mm, maximum stress decreases by -8.68%, but at 300 mm, it increases sharply by 122.97%, highlighting potential instability in stress calculations at coarser meshes. As mesh refines, stress variations decrease, suggesting finer meshes yield more stable and consistent stress calculations, converging towards a reliable solution at 100 mm. In absolute terms, maximum stress at 500 mm is 167.43 MPa, peaking at 407.93 MPa at 300 mm before stabilising around 182.99 to 190.9 MPa in finer meshes. Deflection measurements also increase in accuracy with finer meshes, peaking at 8.1059 mm at the finest mesh compared to 5.4124 mm at the course.

Overall, this analysis highlights the critical role of mesh size in finite element analysis, affecting both accuracy and stability of results. Finer meshes, while more computationally demanding, provide more reliable results in stress and deformation, crucial for assessing structural integrity.
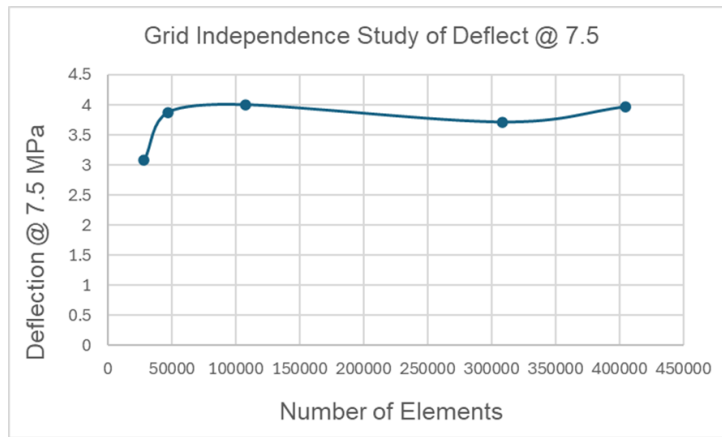
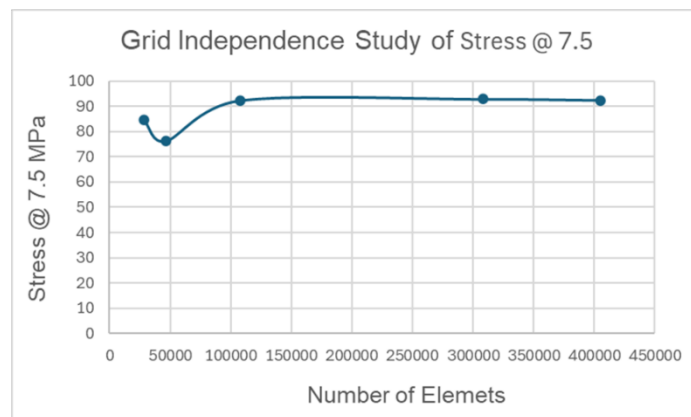**Figure 26:The independence solid convergence study @ deflection 7.5**

Figure 27:The independence solid convergence study @ stress 7.5

The convergence study reveals that as mesh size decreases, deflection and stress metrics generally increase, suggesting finer meshes capture more detailed deformations. The minimal changes between 150 mm and 100 mm meshes indicate an optimal balance, making them suitable for accurate, efficient structural analysis and safety assessments of the tank.

Limitations and Challenges Encountered in the Project

Software Complexity and Coding Challenges.

Using ANSYS Software:

- The use of ANSYS for finite element analysis posed significant challenges, particularly in terms of setting up the model with accurate material properties, loading conditions, and boundary constraints. The complexity of the software required a deep understanding of its capabilities and limitations, making the process time-consuming and prone to errors.

Creating MATLAB Code:

Developing MATLAB scripts for data extraction, rescaling, and RGB-to-thickness conversion involved considerable coding effort. The need to handle large datasets and perform precise mathematical operations added to the difficulty. Ensuring the accuracy and efficiency of these scripts was critical to the success of the project but required substantial debugging and validation efforts.

Data Inconsistencies and Missing Data:

- The corrosion map images provided for the wall thickness analysis had several inconsistencies, including areas with missing data represented by grey or black sections. These missing sections could not be assessed due to inaccessibility, requiring careful consideration in the modelling process to avoid inaccuracies.

Scaling and Alignment Issues:

- The corrosion map strakes were not to scale initially, necessitating rescaling using MATLAB to ensure they reflected the actual dimensions of the tank. This added complexity to the data preparation phase and introduced potential for scaling errors.

RGB-to-Thickness Conversion Errors:

- The conversion of RGB values from the corrosion map to wall thickness data introduced significant errors, especially along the edges of the scan areas. These errors required the application of a moving average filter to smooth out the data, which, while effective, may still not perfectly represent the true wall thickness.

Limited Access to Raw Data:

- Only the minimum wall thickness data for each scan area was provided in a spreadsheet, with no access to the raw full-field phased array ultrasonic thickness (PAUT) scan data. This limitation restricted the ability to perform more detailed and accurate analyses.

Interpolation and Overfitting in ANSYS:

- ANSYS typically uses interpolation or spline fitting to process wall thickness data based on several nearest nodes. While this method is effective for sparse data, it becomes problematic with dense datasets, leading to overfitting and unrealistic thickness variations at each node.

Mesh Element Size and Averaging:

- To accurately represent the wall thickness in the finite element model, the thickness needed to be averaged over an area proportional to the mesh element size. This added an additional layer of complexity and potential for averaging errors.